Optimization of CO_2 injection using multi-scale reconstruction of composition transport

Chen, Yuan; Voskov, Denis

DOI
10.1007/s10596-019-09841-8

Publication date
2019

Document Version
Final published version

Published in
Computational Geosciences

Computational Geosciences (2020) 24:819–835
https://doi.org/10.1007/s10596-019-09841-8

ORIGINAL PAPER

Optimization of CO_2 injection using multi-scale reconstruction of composition transport

Yuan Chen[1] · Denis Voskov[1,2]

Received: 31 October 2018 / Accepted: 30 May 2019 / Published online: 2 July 2019

Abstract

The current situation with green gas emission requires the development of low-carbon energy solutions. However, a significant part of the modern energy industry still relies on fossil fuels. To combine these two contradictory targets, we investigate a strategy based on a combination of CO_2 sequestration with enhanced oil recovery (EOR) in the hydrocarbon reservoirs. In such technology, the development of miscibility is the most attractive strategy from both technological and economic aspects. Modeling of this process involves solving complex nonlinear problem describing compositional flow and transport in highly heterogeneous porous media. An accurate capture of the miscibility development usually requires an extensive number of components to be present in the compositional problem which makes simulation run-time prohibitive for optimization. Here, we apply a multi-scale reconstructing of compositional transport to the optimization of CO_2 injection. In this approach, a prolongation operator, based on the parametrization of injection and production tie-lines, is constructed following the fractional flow theory. This operator is tabulated as a function of pressure and pseudo-composition which then is used in the operator-based linearization (OBL) framework for simulation. As a result, a pseudo two-component solution of the multidimensional problem will match the position of trailing and leading shocks of the original problem which helps to accurately predict phase distribution. The reconstructed multicomponent solution can be used then as an effective proxy-model mimicking the behavior of the original multicomponent system. Next, we use this proxy-model in the optimization procedure which helps to improve the performance of the process several fold. An additional benefit of the proposed methodology is based on the fact that important technological features of CO_2 injection process can be captured with lower degrees of freedom which makes the optimization solution more feasible.

Keywords Operator-based linearization · Reduced model · Optimization · Compositional modeling

1 Introduction

Greenhouse gas emission together with a high demand of energy has long been a concern of contemporary society. Near-miscible CO_2 injection is among the most efficient strategies for a tertiary recovery of oil [16]; it can also effectively reduce carbon emissions. The produced hydrocarbons can be seen as a low-carbon fuel due to the significant amount of CO_2 left in the subsurface as the result of the EOR application. Nevertheless, the heterogeneity of subsurface with complex multi-scale characteristics requires a suitable and highly resolved model to comprehend the details of flow and interactions with the subsurface.

The current economic situation, especially low oil price and formidable cost of CO_2, introduces extra challenges on applying a miscible gas injection. However, in combined objective of enhanced oil recovery and CO_2 sequestration, the development of miscibility may become the most attractive strategy from both technological and economic points of view. In addition, effective miscible injection can increase the storage capacity for CO_2 sequestration in virgin or depleted hydrocarbon fields. It is quite important to develop a plausible techno-economic model to meet the combined goals of oil recovery and carbon dioxide sequestration. This serves as a primary motivation for this study.

To simulate the miscible gas injection process, compositional modeling is inevitably employed. Compositional models require numerical solution of nonlinear equations that involve mass conservation of different components and thermodynamic equilibrium. The phase behavior of

✉ Denis Voskov
D.V.Voskov@tudelft.nl

[1] Stevinweg 1, 2628 CN, Delft, ZH The Netherlands

[2] Stanford University, Stanford, CA, USA

multiphase multi-component mixtures is usually resolved by applying an equation of state (EoS) [2, 3]. A near-miscible gas injection process usually involves a large number of species in solution, which significantly degrades simulation performance. In addition, in nonlinear iterations, thermodynamic equilibrium should be enforced in every grid block to check the phase behavior of the mixture; this adds to the performance penalty [10].

Thermodynamic equilibrium usually consists of two stages: a phase stability test [20] and flash calculation [21]. Various EoS have been used to represent thermodynamic equilibrium in a hydrocarbon mixture, starting with the classic cubic EoS [26, 31]. However, the growing accuracy of reservoir fluid characterization and better recognition of complex physical processes involving component interactions requires an application of a more complicated EoS, such as statistical associating fluid theory (SAFT) [1] or cubic-plus-association (CPA) [14]. In addition, coupling with chemical reactions requires a combination of thermodynamic and chemical equilibria [17, 24]. This can significantly increase the cost of phase-behavior computations in compositional simulation [34].

Several efforts have been made to improve the performance of compositional reservoir simulators by improving phase-behavior computations [9, 23, 28, 35], spatial coarsening of compositional models [8, 30], or reformulation of compositional nonlinear problem [38]. In this work, a newly proposed multi-scale reconstruction in physics (MSRP) approach by [6] is utilized for production optimization. The algebraic multi-scale (AMS) approach was initially proposed to solve an elliptic flow problem in [11]. Several extensions of this method have been successfully developed. However, most of the AMS methods were focused exclusively on the flow solver and did not address the transport problem, except [39], where an adaptive multi-scale finite volume method was proposed to accelerate the transport solver. On the basis of these ideas, an MSRP method for reconstruction of the compositional transport problem with an arbitrary number of components was developed in [6].

This approach suggests a two-stage reconstruction, where, at the first stage, the boundary of a two-phase region is recovered, and the detailed solution in the two-phase region is reconstructed in the second stage. The MSRP approach utilized an operator-based linearization (OBL) technique proposed in [36]. In the OBL method, the terms of the discretized governing equations are factorized into space- and state-dependent operators. The state-dependent operators are adaptively discretized in the parameter space of the problem, and multi-linear interpolation is applied for continuous representation [13]. This formulation helps to avoid the performance issues associated with an accurate phase-split evaluation and reduces the nonlinearity of the problem. Recently, this approach was extended for adaptive parametrization of thermal-compositional problems with buoyancy [12].

The original study of the MSRP method was limited to isothermal two-phase flow with fixed phase-equilibrium ratios (K values) [5]. In this work, we introduce an application of MSRP using the Peng-Robinson equation of state [26]. Due to the strong nonlinearity of the CO_2 injection system, constrained nonlinear optimization strategy is utilized to determine the optimal production scenario. For production optimization, we used only the first-stage MSRP reconstruction as a physics-based proxy model and compare its result with optimization of the full compositional solution. Both approaches were compared using an idealized conceptual model with growing optimization complexity.

2 Model description

In this section, a concise simulation framework based on [36] is presented.

2.1 Compositional framework

For simplicity, the thermal changes, capillarity, gravity, and diffusion are neglected in the following description. The general mass conservation equation for component i in the two-phase compositional problem is defined as follows:

$$\frac{\partial}{\partial t}\left(\phi \sum_{j=1}^{2} x_{i,j}\rho_j S_j\right) + \nabla \cdot \sum_{j=1}^{2} x_{i,j}\rho_j \mathbf{u_j} + \sum_{j=1}^{2} x_{i,j}\rho_j q_j = 0, \quad i = 1, ..., N_c \tag{1}$$

In (1), t is time, ϕ is the porosity of the reservoir, ρ_j is molar phase density, S_j is phase saturation, $x_{i,j}$ is the mole fraction of component i in phase j, q_j is the source or sink term of phase j, and N_c is number of the components. The Darcy velocity $\mathbf{u_j}$ is defined as follows:

$$\mathbf{u_j} = -K\frac{k_{\mathrm{rj}}}{\mu_j}\cdot\nabla p, \quad j = 1, 2, \tag{2}$$

where K is absolute permeability, k_{rj} is the relative permeability of phase j, μ_j is viscosity of phase j, and p is pressure. The equilibrium relations between oil and gas phase are required to close the system as follows:

$$\hat{f_{i,o}}\left(p, T, \mathbf{x_0}\right) = \hat{f_{i,g}}\left(p, T, \mathbf{x_g}\right), \quad i = 1, ..., N_c, \tag{3}$$

where $\hat{f_{i,o}}$ and $\hat{f_{i,g}}$ are the fugacities for the component i in oil phase and gas phase, respectively. Fugacity is a function of pressure (p), temperature (T), and phase compositions ($x_{i,j}$), which are determined by EoS-based

flash computations. Additional equations are given as follows to close the system of governing equations:

$$\sum_{i=1}^{N_c} \left(x_{i,1} - x_{i,2}\right) = 0, \quad i = 1, ..., N_c, \tag{4}$$

$$s_o + s_g = 1. \tag{5}$$

The overall composition of i component can be expressed as follows:

$$z_i = \sum_{j=1}^{2} v_j x_{i,j}, \quad i = 1, ..., N_c, \tag{6}$$

where v_j is the molar fraction of the phase $j(o, g)$. Solving the Eq. (3) is a procedure called multi-phase flash [21], which will provides phase composition $x_{i,j}$ and phase fraction v_j. Finally, the phase saturation s_j can be found from the following:

$$s_g = \frac{v_g}{\rho_g} / \left(\frac{v_g}{\rho_g} + \frac{v_o}{\rho_o}\right) \tag{7}$$

Applying two-point finite volume in space and backward Euler in time discretizations, the general mass conservation equation is written as follows:

$$V\left(\left(\phi \sum_{j=1}^{2} x_{i,j}\rho_j S_j\right)^{n+1} - \left(\phi \sum_{j=1}^{2} x_{i,j}\rho_j S_j\right)^{n}\right)$$
$$-\Delta t \sum_{l\in\mathbf{L}} \left(\sum_{j=1}^{2} x_{i,j}^{l}\rho_j^{l} T_j^{l} \Delta\Psi^{l}\right) + V\Delta t \sum_{j=1}^{2} x_{i,j}\rho_j q_j = 0, \tag{8}$$

where V is total control volume and $\mathbf{L}$ represents the interface which connects the control volume with another grid blocks. In the simplified assumptions mentioned above, ϕ is porosity, $\Delta\Psi^{l}$ becomes a pressure difference between two connected grid blocks. Finally, T_j^{l} is the transmissibility of phase j.

In our conceptual model, we ignored gravity, capillarity, and thermal variations focusing mostly on compositional effects. These assumptions were applied to simplify the analysis of optimization results which focus mostly on compositional effects in CO_2 injection process for EOR and sequestration. All these phenomena may increase the complexity of proxy-model, which will be considered in our future research. Notice that the OBL approach was already extended for problems with buoyancy in [12].

2.2 Operator-Based Linearization

The multi-scale technique is implemented on the basis of an OBL approach proposed by [36]. To apply OBL, the discretized mass conservation equation (8) is written in the following residual form:

$$r_i\,(\xi, \omega, \mathbf{u}) = a\,(\xi)\,(\alpha_i\,(\omega) - \alpha_i\,(\omega_n)) - \sum_{v} \beta_i^{v}(\omega) b^{v}(\xi, \omega)$$
$$+\theta_i(\xi, \omega, \mathbf{u}) = 0 \tag{9}$$

The operators in Eq. (9) are defined as follows:

$$\alpha_i\,(\omega) = (1 + c_r\,(p - p_{\text{ref}})) \sum_{j=1}^{2} x_{i,j}\rho_j S_j, \tag{10}$$

$$a\,(\xi) = V(\xi)\phi_0(\xi), \tag{11}$$

$$\beta_i(\omega) = \sum_{j}^{2} x_{i,j} \frac{k_{\text{rj}}}{\mu_j}\rho_j, \tag{12}$$

$$b(\xi, \omega) = \Delta t T_{\text{ab}}(\xi)(p^{b} - p^{a}), \tag{13}$$

$$\theta_i(\xi, \omega, \mathbf{u}) = \Delta t \sum_{j=1}^{2} x_{i,j}\rho_j q_j(\xi, \omega, \mathbf{u}). \tag{14}$$

In Eqs. (10) to (14), c_r is rock compressibility and T^{ab} is the transmissibility between grid blocks. The vector $\mathbf{u}$ contains well-control variables, ω is the set of state variables and ξ are the set of spatial coordinates. In addition, α_i is the accumulation operator, β_i is the flux operator, and θ_i is the source/sink operator. The OBL approach is based on a simplified representation of the nonlinear operators in the parameter space of the simulation problem. For an isothermal reservoir simulation, the parameter space is defined by the range of pressure (p) between injection and production conditions and overall compositional (z_i) range from 0 to 1. The fully implicit method (FIM) is utilized for time approximation, and Newton-Raphson method is applied to solve the governing equation Eq. (9) based on the set of nonlinear unknowns.

2.3 Multi-scale compositional transport

A solution of a compositional transport problem can be shown in a phase diagram by the solution path in compositional space, which defines the compositional changes between the initial and injection mixtures. Conservation principles and fractional flow theory form the foundation for the general solution method [22]. The compositional path of the conventional compositional problem for gas injection process, when the injection mixture is a single-phase gas and initial fluid is a single-phase liquid, always results in two shocks (leading and trailing shocks) between single- and two-phase regions. In a ternary diagram (Fig. 1a), it is presented as yellow lines connecting the initial oil and injected gas composition.

The shocks between single- and two-phase regions are always aligned along two key tie-lines (black-dashed lines) defined by liquid x_i and vapor y_i fractions of each

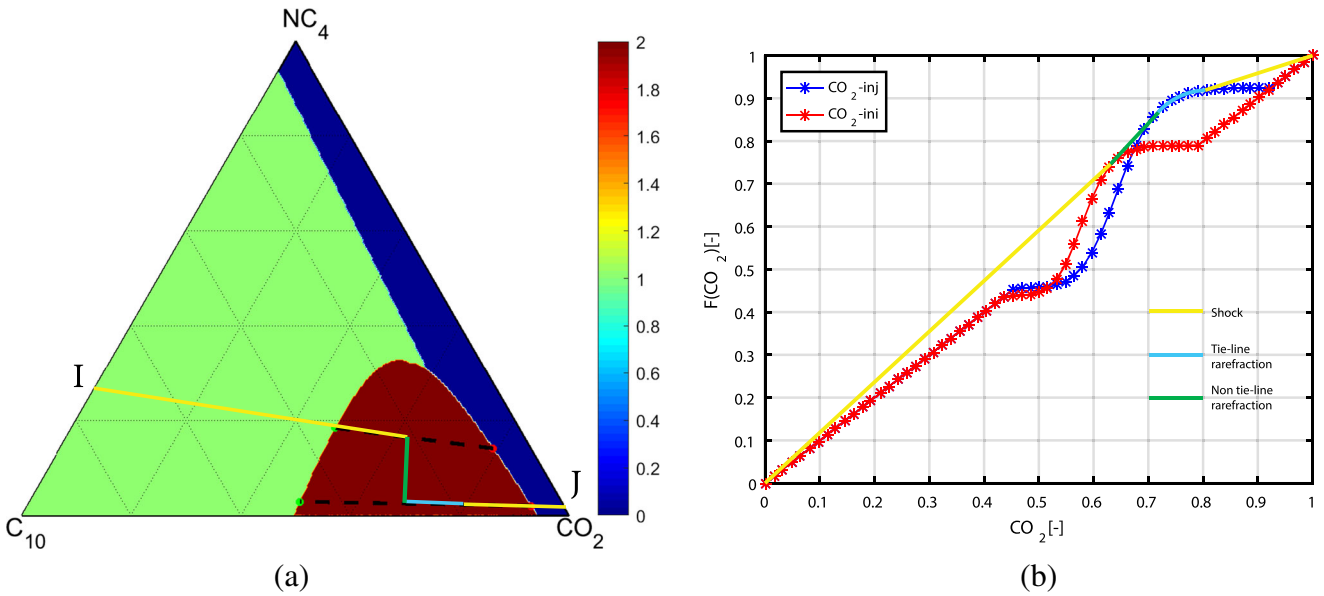

Fig. 1 Gas injection solution in ternary system: **a** ternary diagram with displacement path and two key tie-lines and **b** fractional flow curves for component CO_2 with solution path

component. For a fixed pressure, x_i and y_i remain constant, and it is possible to construct the fractional-flow curve corresponding with compositional transport (see, Eq. (15)). Figure 1b shows the projection of the solution to fractional flow curve for CO_2 component with leading and trailing shocks (yellow) connecting tangent points on initial (red) and injection (blue) fractional flow curves respectively [22]. Note that these curves corresponds with the injection and initial tie-lines in Fig. 1a following the relation:

$$F_i = x_i\left(1 - f_g\right) + y_i f_g, \quad i = 1, ..., N_c - 1. \tag{15}$$

The proposed multi-scale compositional transport approach consists of two stages [5]. The first stage utilizes the set of restriction-prolongation operators for reconstructing two-phase boundaries (the trailing and leading shocks). The restriction here reduces the $n_c - 1$ transport equations to a single equation with a special flux operator based on the pseudo-fractional flow curve. In the second stage, the set of restriction-prolongation operators is applied in the two-phase region to reconstruct the solution structure of the two-phase displacement. This stage is based on the invariance of two-phase solutions in tie-line space reported in [33] and adapted for practice in [35].

The proxy model for compositional simulation, utilized in this work, uses the first-stage multi-scale reconstruction from [5]. A restriction operator combines two fractional-flow curves for injection and production tie-lines (red and blue curve from Fig. 1b), defined as follows:

$$F_I^{\text{ini}} = x_I^{\text{ini}}(1-f_g)+y_I^{\text{ini}} f_g, \quad F_I^{\text{inj}} = x_I^{\text{inj}}(1-f_g)+y_I^{\text{inj}} f_g. \tag{16}$$

The equivalent fractional flow curve (green in Fig. 2), serving as the restriction operator, is constructed by taking a convex hull on the union of both curves.

$$F_R = \text{conv}(F_I^{\text{inj}} \cup F_I^{\text{ini}}). \tag{17}$$

This means that the green line in Fig. 2 repeats the fractional flow curve for the initial tie-line starting from the left and switches to the injection tie-line in the intersection point. Next, the equivalent values of F_i and z_i from the green curve are tabulated into the restriction operator and the reduced system is solved. The reduced system of equations contains the restricted transport equation based on the

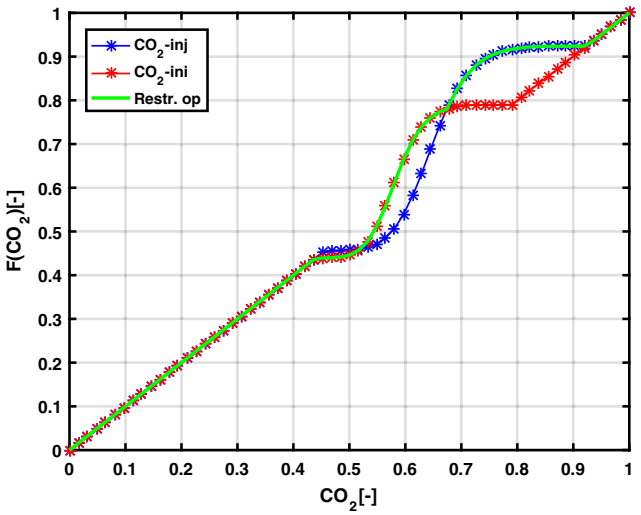

Fig. 2 Analytical fractional flow for CO_2

constructed pseudo-fractional flow curve. Notice that by structure, this system is very close to the conventional binary compositional problem.

Once the solution of the restricted system is found, the full system is reconstructed based on the prolongation operator. This operator applies interpolation for all components in the solution between initial and injection compositions using the solution of the restricted system $\kappa(z_R)$ (corresponds to the CO_2 component in this example) as an indicator:

$$\kappa(z_R)\left[\mathbb{R}^1 \Longrightarrow \mathbb{R}^{n_c-1}\right] : \mathbf{z} = \mathbf{I}_{\{z^{\text{ini}}, z^{\text{inj}}\}}(z_R). \tag{18}$$

Here, κ is the interpolation-prolongation operator, z_R is the restricted solution, and $\mathbf{I}$ is the piecewise linear interpolation function. Referring to this linear interpolation, the transport solution of other components in the multicomponent system is reconstructed and used as a proxy model in place of the full compositional model. Notice that this system can accurately predict only the boundaries of the two-phase region and their dynamic propagation in space; for a really accurate solution, the second-stage multi-scale reconstruction should be applied [5].

3 Economic model

The techno-economic model is applied to evaluate the economics of a combined CO_2 EOR and sequestration application. Several economic studies of CO_2 injection processes have been performed in [4, 15, 29, 32]. McCoy and Rubin [19] proposed several regression equations for assessment of the capital cost of CO_2 injection projects, which are validated in [37] and [4]. Referring to [32], this techno-economic model uses simulation input data and oil production rate, gas injection rate, and bottom hole pressure (BHP) to define different costs and revenues of the project.

On the basis of reservoir-simulation data, an economic model is developed to estimate the profitability of CO_2 injection for enhanced oil recovery (EOR) and CO_2 sequestration, which will reflect on the net present value (NPV). The general economic parameters of a CO_2 injection process are listed in Fig. 3.

This figure shows that the cost of a CO_2 injection project can be divided into two parts, which are capital cost and operational cost. Dominant revenues from the gas injection project mainly originate from oil sales and carbon sequestration incentives. A previous economic study of CO_2 injection projects [15] indicates that CO_2 purchasing cost is one of the most sensitive parameters when NPV is evaluated.

In this work, we identify that CO_2 processing cost has a similar impact on NPV as CO_2 purchasing cost. The CO_2 processing cost model in this work is based on [32], and is expressed in terms of the pump capital cost as follows:

$$C_{\text{pump}} = \left(1.35 \times 10^3 \times W_p\right) + 0.085 \times 10^6, \tag{19}$$

where W_p is pumping power requirement, which is expressed in kW, which in turn varies with CO_2 injection pressure. Other parameters in the economic model are listed in Table 1. Some of them are obtained by introducing the regression equations listed in [19], such as those for well engineering cost and CO_2 processing equipment cost.

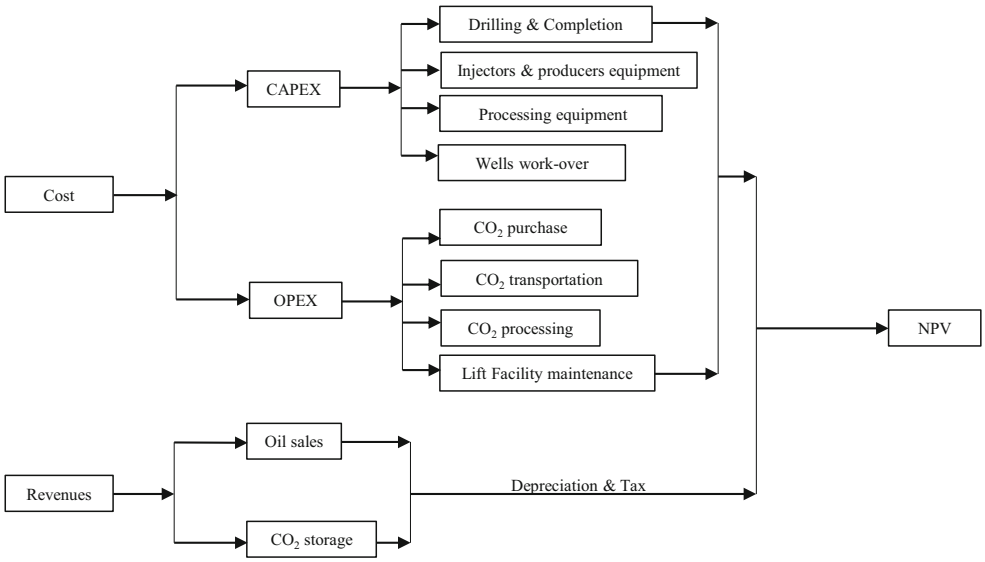

Fig. 3 General economic parameters for CO_2 injection project

Table 1 The values for economic parameters

Parameters		Units	Remarks
CO_2 storage incentives	50	\$/t	[19]
Well engineering cost	501644	\$	[19]
CO_2 processing equipment	10637265	\$	[19]
Wells work-over	241429	\$	[19]
CO_2 purchase cost	24	\$/t	[15]
CO_2 transportation	0	\$/t	CO_2 source in situ
CO_2 processing cost	10	\$/t	[29]
Lift facility maintenance	0.6	\$/t	[29]
Tax rate(royalty, severance tax)	0.4	[-]	[19]
Depreciation	Linear over 10 years	\$	
Discount rate	12	[–]	[37]

4 Numerical results

In this section, we demonstrate the comparison between solutions of the proxy model and the full compositional model. Here, we limit our investigation to a conceptual 1D reservoir model for simplicity of the optimization results interpretation. In this model, the injection well on the left operates at a constant gas rate when the production well is controlled by BHP which serves as a control variable for optimization.

4.1 Restricted solution

Figure 4 shows the estricted solution z_R, which yields the shock reconstruction curves for simulation results for the growing BHP at the production well. All simulation results are shown for the model with parameters specified in Appendix A. The K-value table in this work is obtained from the embedded constant composition expansion (CCE) experiments in [7] based on the PR EoS, which is shown in Tab 10. It is clear that the K value system does not develop miscibility even when BHP provides the pressure at the displacement front close to the first-contact minimal miscibility pressure (FC MMP) for this system (around 126 bars at T = 373K). This happens due to the inability of the K-value model to predict miscibility accurately, since compositional dependency is not captured in this model.

It can be overcome by either extension of the K value parameterization with additional degrees of freedom, e.g. [27], or incorporation of EoS-based phase behavior [2]. However, it is clear that the two-phase boundaries can be accurately represented by the restricted model for K-value-based physics. In addition, the complexity and structure of the restricted solution are invariant with respect to the number of components present and only depends on initial and injection tie-lines in the multicomponent system (see, [5] for details).

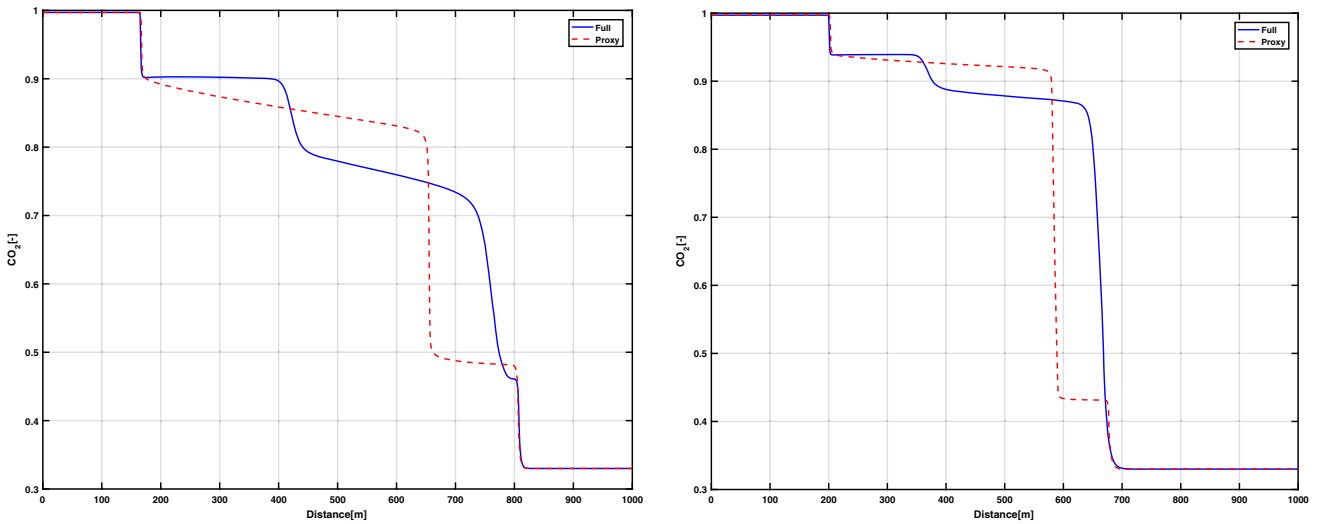

(a) Restricted solution-BHP=85bars (b) Restricted solution-BHP=120bars

Fig. 4 Shock reconstruction of the four-component system for two different BHP controls at production well (K values)

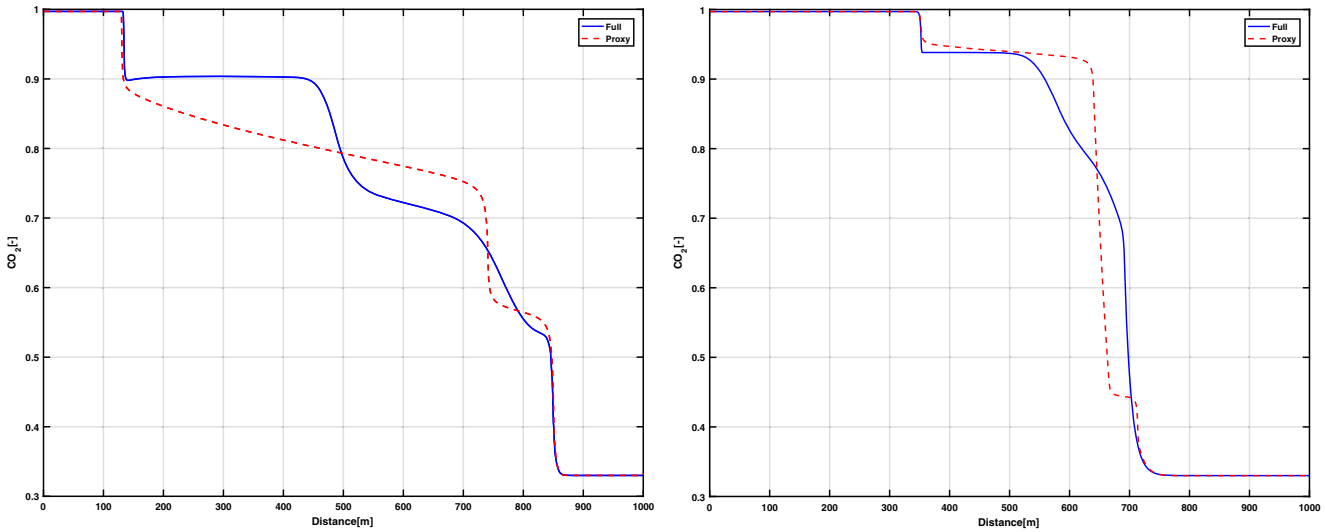

(a) Restricted solution-BHP=85bars (b) Restricted solution-BHP=120bars

Fig. 5 Shock reconstruction of the four-component system for two different BHP controls at production well (EoS model)

Next, the results of the restricted solution for the compositional problem based on the EoS is shown. The structure of the compositional transport solution depends on key tie-lines [22]. For the restricted solution, we follow the same strategy as before and construct the restriction operator based on combined fractional flow (16) according to the first stage of MSRP approach [5]. The solution of the restricted transport equation reconstructs the boundaries of the two-phase region using one transport equation instead of $n_c - 1$ equations in the conventional compositional model.

The results of quaternary system reconstruction are shown in Fig. 5. Here, you can see that for a high BHP value, the structure of the solution is much closer to miscibility (leading and trailing shocks stays closer to each other) than in the K-value approximation. This happens because the EoS-based phase behavior correctly represents the compositional dependency of the solution. Similar to the K-value model, the restriction stage requires the solution of only one equation instead of $n_c - 1$, where n_c is the number of components.

Next, we present the simulation results for more realistic multicomponent mixture. Here, we used the eight-component system from [38] with compositional parameters shown in Table 9 (see Appendix). In cooperating

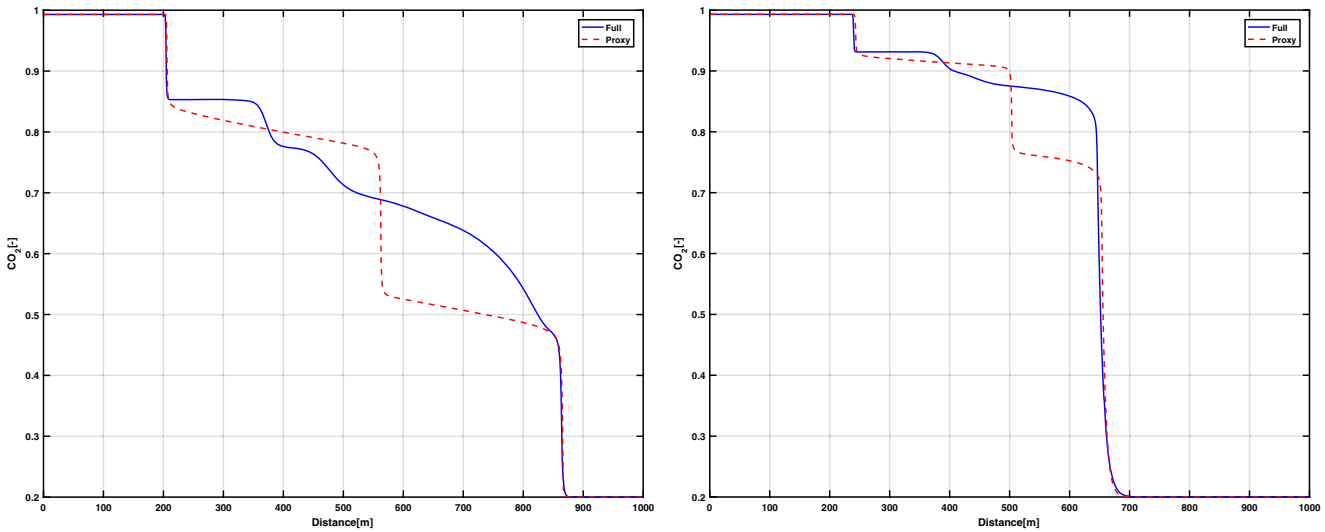

(a) Restricted solution for BHP = 80 bars (b) Restricted solution for BHP = 140 bars

Fig. 6 Shock reconstruction of the eight-component system for two different BHP controls at production well (K values)

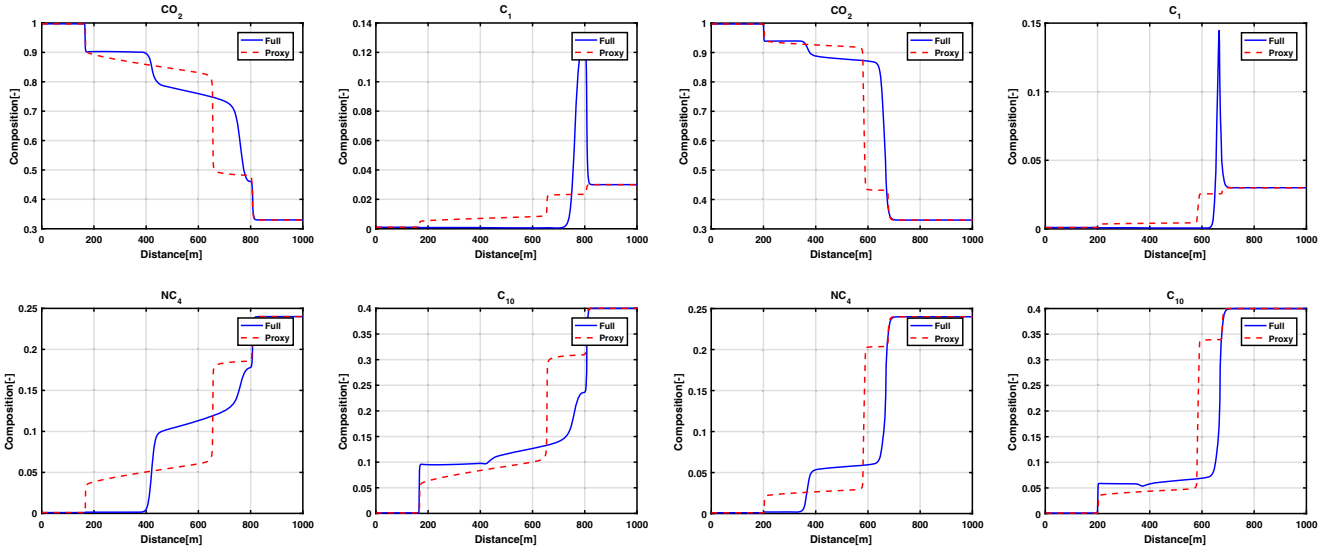

(a) Full solution-BHP=85bars (b) Full solution-BHP=120bars

Fig. 7 Proxy model for a four-component system (K-value based)

with the K values generated using [7], and shown in Table 11, the restricted solution based on the first-stage reconstruction of MSRP approach, is present in Fig. 6.

4.2 Prolongation of proxy model

Here, we illustrate the construction of the proxy model using an interpolation-based prolongation operator Eq. (18) for both restricted solutions from 4.1. It can be seen in Figs. 7 and 8 that the prolongation operator does not reconstruct the full structure of the solution but only one indicator component. However, the prolongation yields a full compositional solution in every control volume, which then can be used in a multiphase flash procedure to predict phase behavior. This procedure provides the boundary of the two-phase region in space.

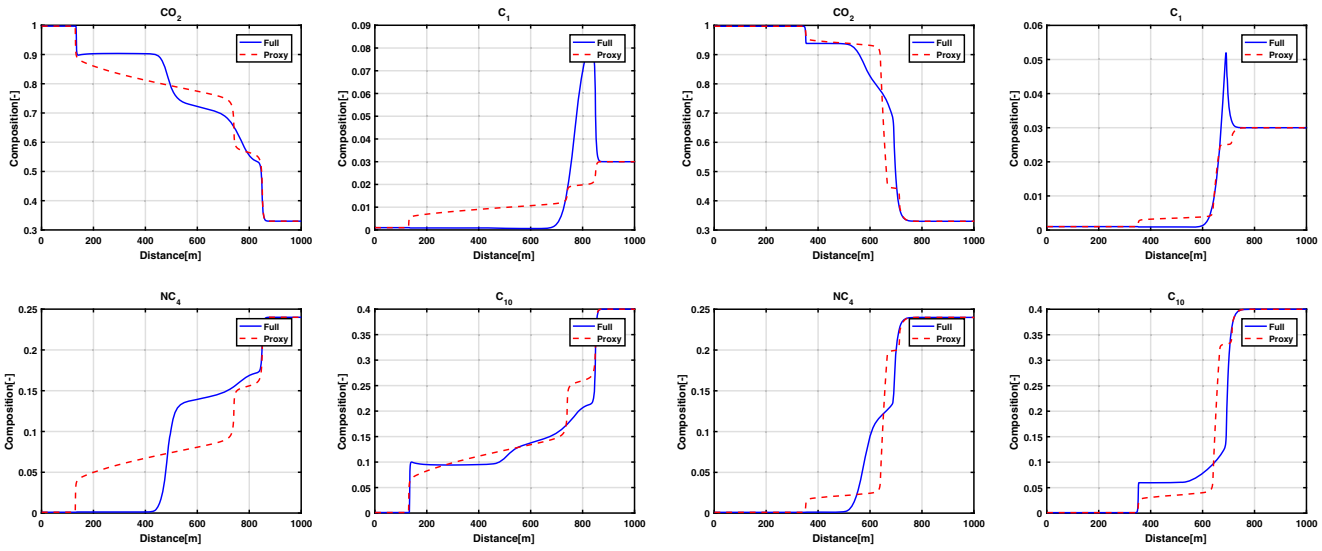

(a) Full solution-BHP=85 bars (b) Full solution-BHP=120 bars

Fig. 8 Proxy model for a four-component system (EoS based)

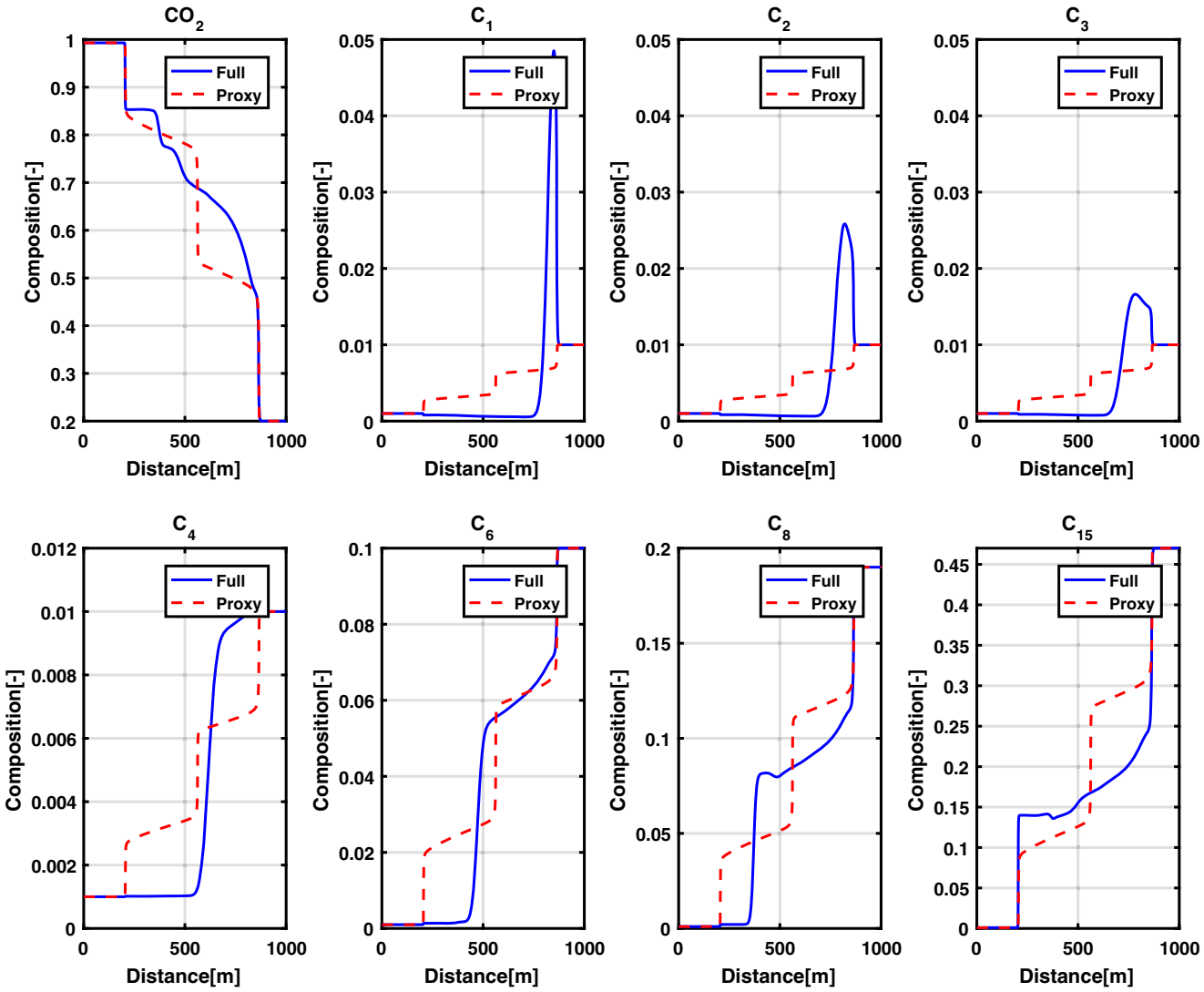

Fig. 9 Proxy model for an eight-component system (K-value based); BHP = 80 bars

Next, we construct the proxy model for the eight-component case. Similarly to a previous case, we apply an interpolation-based prolongation operator Eq. (18) for K values system which yields the first-stage MSRP approach shown in Figs. 9 and 10 for given two BHP values 80 bars and 140 bars respectively. The compositions of these components and K-value tables are shown in the Appendix (Tables 9 and 11). This proxy model still cannot recover the full solution of the eight-component model and the second-stage MSRP approach should be employed to reconstruct the solution in two-phase region (see details in [5]).

The prolongation yields a full compositional solution at every grid block, which then can be used in a multiphase flash procedure to predict phase behavior. This provides an accurate reconstruction of the two-phase boundaries. In our proxy model, we are using this prediction to compute phase rates at wells. As a result, this proxy model will be applied to evaluate economic performance of the CO_2 injection project together with full eight-component model in terms of NPV.

5 Conceptual optimization problem

Figure 11 shows the transport solution for both fully compositional and proxy models for different BHP controls at the production well and a fixed rate at the gas injection well. It is clear that with increasing pressure, both models capture the development of miscibility since the BHP control at the production rate will apparently control the pressure at the displacement front. Due to the development

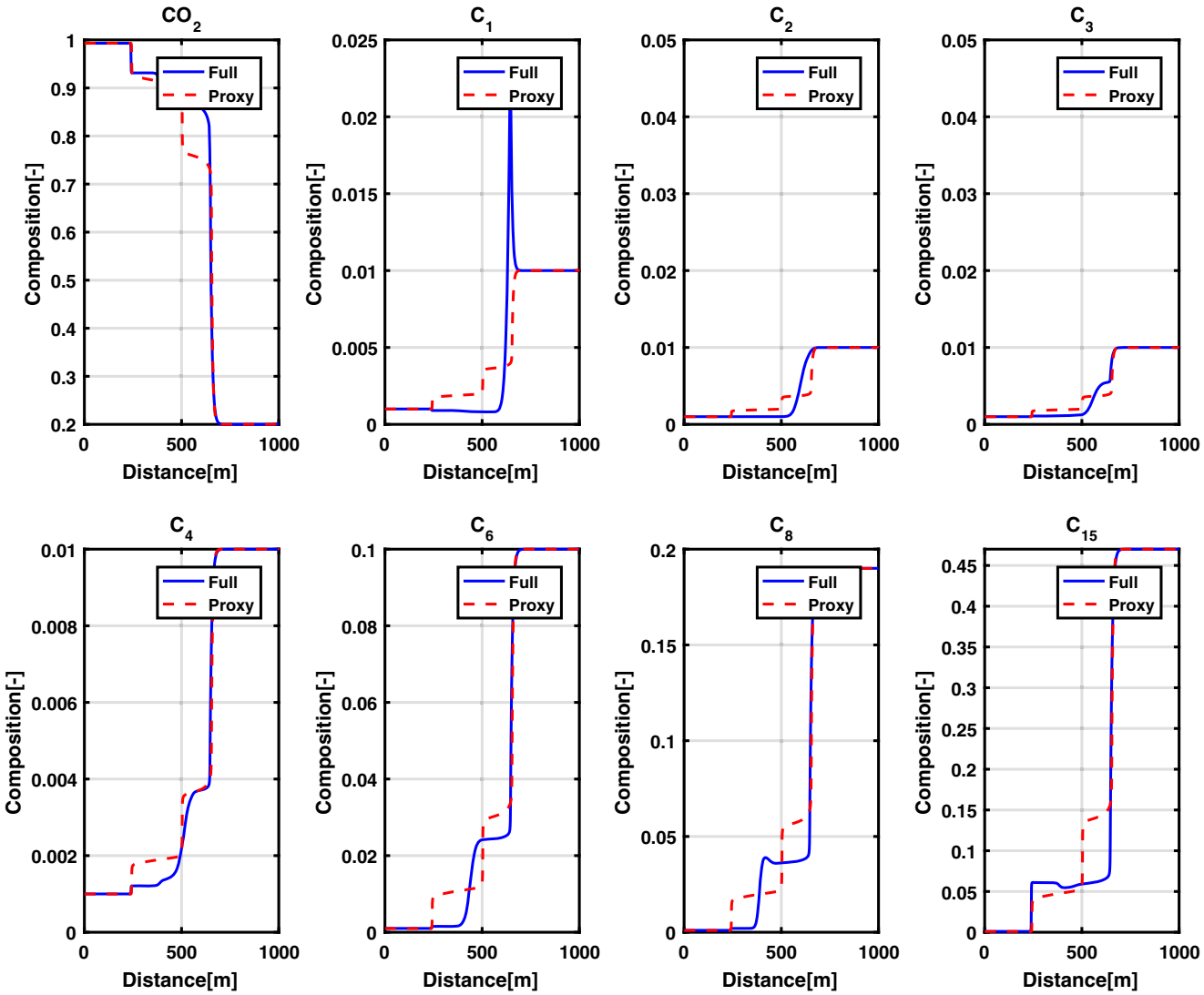

Fig. 10 Proxy model for an eight-component system (K-value based); BHP = 140 bars

of miscibility, the leading and trailing shocks get closer to each other and the displacement efficiency grows. Next, we investigate optimal production strategies for this model.

In the optimization stage, the full four-component system together with the proxy two-component system is used to determine oil production. Net present value (NPV) is used as an indicator to estimate the economic profitability of the project. The simulation time is divided into several periods where changes in BHP at the production well are applied. Here, we make sure that the time period for simulation covers the breakthrough of the trailing shock at the lower limit of pressure. Next, we estimate the optimal production strategy with a different numbers of control variables.

5.1 NPV with a limited number of control parameters

The NPV distribution as a function of a single BHP control is evaluated here. We compare the NPV curve vs. BHP control for both the proxy and the full compositional model. The simulation time is defined to be long enough for the breakthrough of both leading and trailing shocks of the solution. The NPV plotted as a function of control BHP is shown in Fig. 12.

Here, the green solid curve is the NPV results from the full four-component model, and the red-dashed curve is the NPV results from the proxy model. While there are some discrepancies in the proxy solution due to the limited application of the MSRP (only first stage of reconstruction),

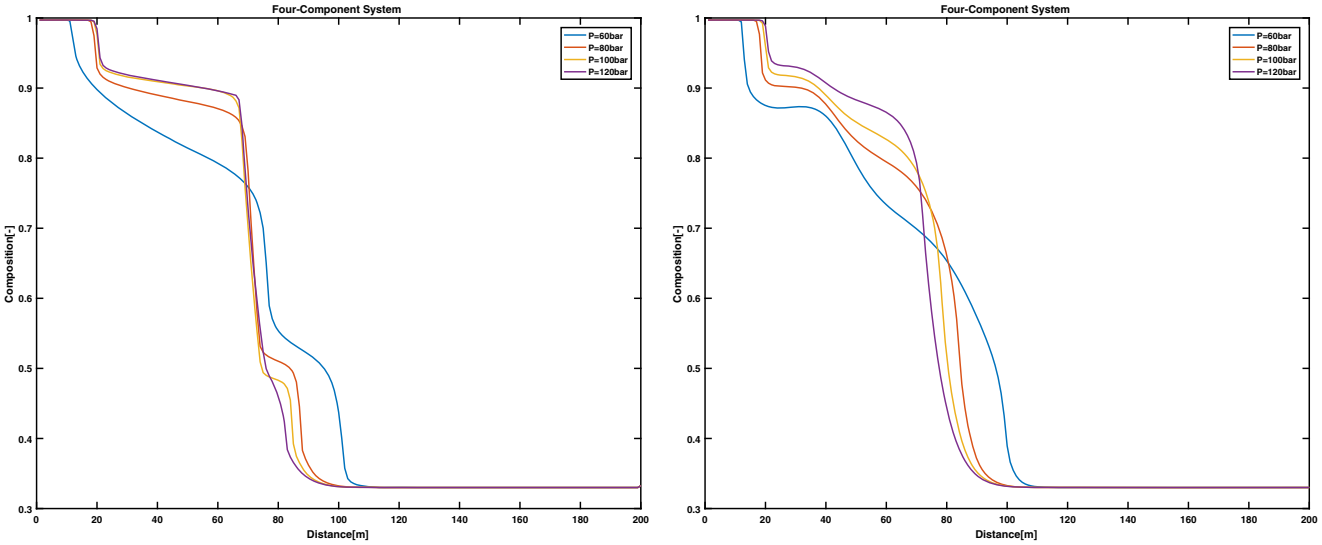

(a) Four-component transport (T = 1000days) (b) Two-component transport (T = 1000days)

Fig. 11 Transport solution and pressure profile for five different BHP controls at the producer

the model captures the correct boundaries of the two-phase region and yields the correct maximum of the NPV function. To reduce the differences in NPV evaluation, the second stage of the MSRP reconstruction can always be performed.

Notice, that this behavior is expected. In most of current gas injection projects, the cost of CO_2 remains a major factor for project economy. In our model, the simplified physical assumptions and CO_2 sequestration credits yield the development of miscibility as an optimal strategy to improve NPV. The BHP corresponding to the maximum value of NPV in Fig. 12 is located close to the minimal miscible pressure of this system which is followed by the NPV reduction due to the growing cost of pumping. The majority of proxy models for gas injection problems poorly approximate the development of miscibility which requires an application of high-fidelity compositional models. We demonstrate that our proxy model is able to capture the near-miscible behavior and correctly identify the maximum of the NPV.

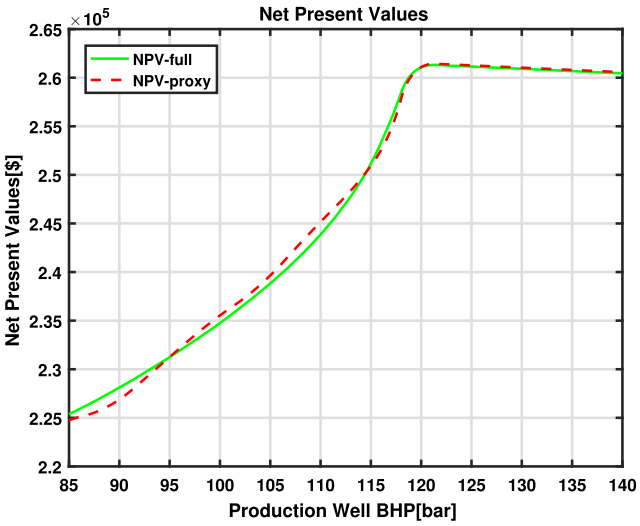

Fig. 12 NPV with one control parameter

Next, we introduce two simulation time periods and two control variables (BHP_1 and BHP_2) for NPV evaluation. For this situation, the prediction of optimal controls for both periods is not as simple as in the previous example. Performing an exhaustive search in the space of control variables, we evaluate the NPV function (shown in Fig. 13). While the NPV function is different for the proxy and the full model, the maximum NPV is reached at the same control values, i.e., around $BHP_1 = 95$ bars and $BHP_2 = 118$ bars. These values are conditioned by the obvious strategy for production controls when in the first-time interval, the lower BHP at the production well provides the near-miscible pressure at the displacement front. In the second-time interval, the higher pressure at the production well provides near-miscible pressure until the breakthrough to the production well. The near-miscible strategy is optimal since it maximizes the oil recovery and sequestrationof CO_2.

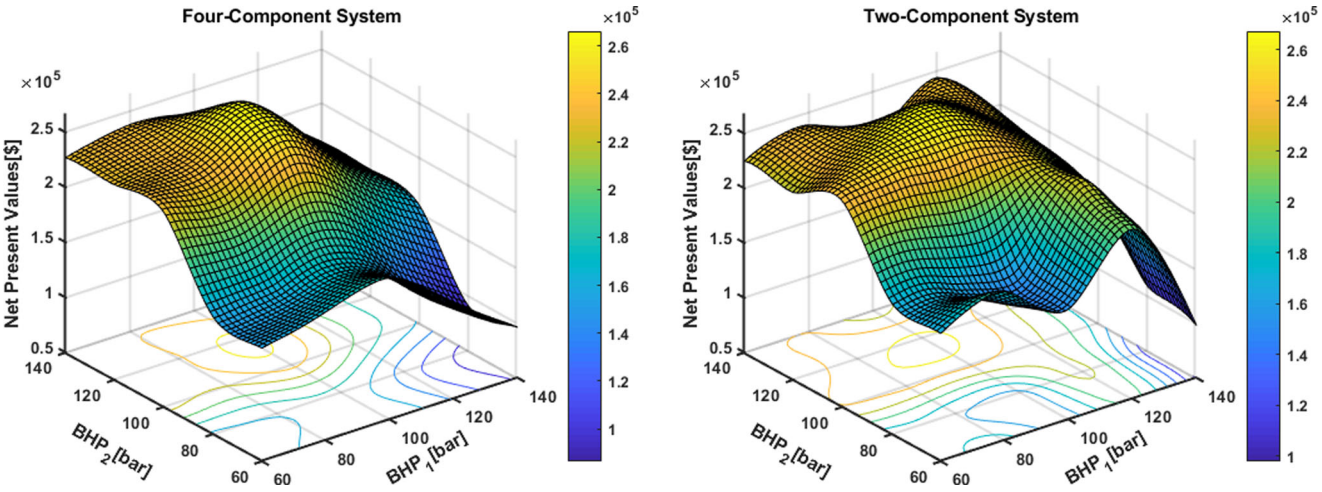

(a) Full model (b) Proxy model

Fig. 13 NPV with two control parameters

In order to illustrate optimization procedure, the optimization trajectory is constructed. Figure 14 gives the result of the optimization trajectory for the full physics model and proxy model respectively. For the proxy model, the number of optimization steps is less than that of the full physics model. In addition, it is faster for the proxy model to acquire a near optimal NPV result with the same optimization strategy. Table 2 presents more details of both optimization runs.

Next, we look into the form of the NPV function for the more realistic eight-component system with compositions and corresponds thermodynamic characteristics shown in the Appendix (Tables 7 and 9). The objective function for two control variables is shown in Fig. 15.

The pressure interval is corresponding to the lower and upper limit of the BHP values of the production wells, which range from 80 to 160 bars. In this eight-component system, given the similar optimal pressure sets for both proxy and full physics model, both models capture the similar highest NPV value. The result is shown in the Table 3.

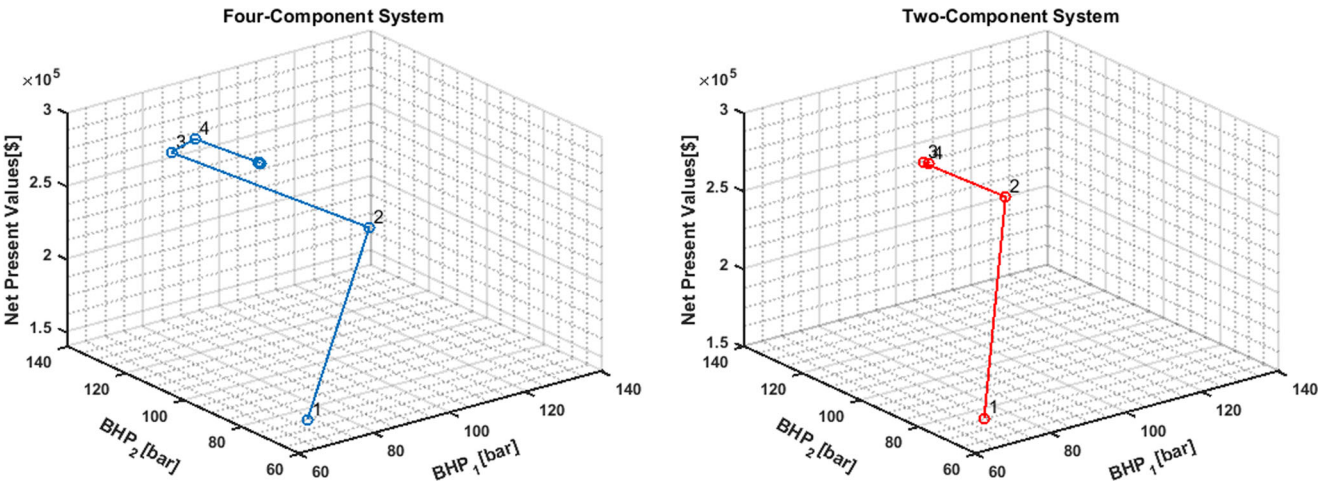

(a) Full model (b) Proxy model

Fig. 14 Optimization trajectory for quaternary system

Table 2 Optimization results for two constant initial BHP

Initial guess	Model	# of iter.	NPV($)	Controls for time periods	
				1	2
BHP = 70 bars	Full model	14	260,927	94.85	118.55
	Proxy model	5	260,866	94.83	120.41

Table 3 NPV result and optimal pressure sets for an eight-component system

Model	NPV($)	Controls for time periods	
		1	2
Full model	279,576	100 bars	138 bars
Proxy model	279,866	100 bars	137 bars

5.2 Optimization with multiple controls

Next, we apply production optimization based on five control variables (BHPs) corresponding to five time periods in the simulation. In this study, we use the "fmincon" function from the Matlab optimization toolbox [18]. In "fmincon," the "sqp" algorithm has been chosen. The optimizer is utilized to provide BHP controls at each time period and obtain an optimal NPV result during the CO_2 injection process. All BHP controls were bounded by $BHP_{min} = 60$ bars and $BHP_{max} = 140$ bars. Note that the expected optimal strategy should include a gradual increase of BHP at each consecutive control interval to provide near-miscible conditions at the displacement front.

We test several initial guesses for the optimization with five control parameters. For this number of controls, several local minima can exist and the optimizer struggles with finding a single global extremum. However, based on the structure of solution in Fig. 11, we can predict a near-optimal BHP strategy where BHP should monotonically increase with time to provide the near-miscible pressure at the displacement front. Using this strategy with BHP = [63; 77; 83; 102; 121] at five controls intervals as the initial guess, we perform the optimization. The results of optimization based on the full and proxy models are present in Table 4. You can see that the proxy model performed fewer iterations and obtained a similar NPV.

In addition, we perform two more optimization runs with different initial guesses when all BHP controls have been set to 70 bars and 100 bars respectively. The results can also be seen in Table 4. In these optimization runs, both models cannot converge to the same optimal strategy but get close to it. The proxy model performs quite robustly and proves to be applicable for optimization of gas injection process in the idealistic reservoir.

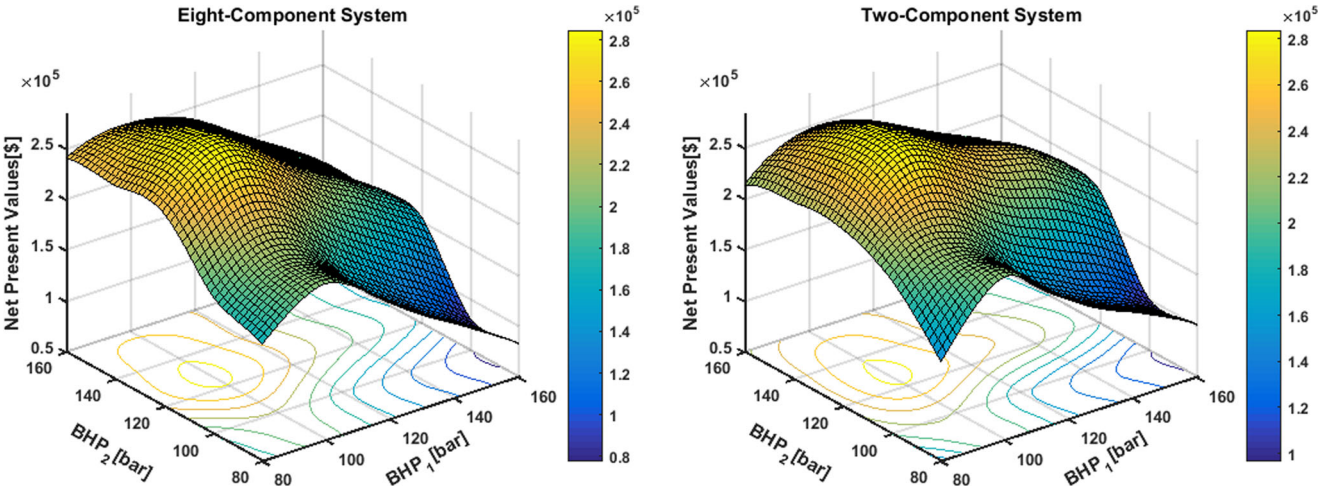

(a) Full model (b) Proxy model

Fig. 15 NPV with two controls: eight-component system

Table 4 Optimization results for constant initial BHP

Initial guess	Model	# of iter.	NPV($)	Controls for time periods				
				1	2	3	4	5
Near optimal	Full model	6	261,100	60.00	76.18	79.21	88.21	117.65
	Proxy model	3	261,064	60.00	76.08	80.07	85.00	117.99
BHP = 70 bars	Full model	11	261,007	60.00	79.33	90.76	63.02	126.11
	Proxy model	12	260,247	60.97	60.05	89.62	117.41	127.74
BHP = 100 bars	Full model	9	260,093	60.00	87.86	107.42	82.86	121.16
	Proxy model	7	260,817	60.00	95.05	105.73	61.97	118.87

6 Conclusions

In this work, we extend the multi-scale reconstruction in physics (MSRP) approach for the EoS-based gas injection problems. In particular, we parametrize the restriction operator of the first-stage MSRP reconstruction in the pressure interval and obtain the restricted solution using the operator-based linearization framework. The restricted solution was prolongated to the full compositional solution using interpolation operator. The obtained proxy model can accurately predict the boundaries of the two-phase region and has been utilized in this work for production optimization in a simplified physical assumptions of the forward problem.

Referring to previous economic assessments of CO_2 injection projects, a techno-economic model has been developed to analyze the revenues of CO_2 injection for the combined objective of EOR and sequestration. A general application of the proposed proxy model for optimization of gas injection process is demonstrated in this study. Starting with a limited number of controls, we show that the objective function of the full physics compositional model and the proposed proxy model share similar extrema for a limited number of control parameters. To test the robustness of the proposed proxy model in relatively complicated cases, the general form of the objective function was evaluated for a limited number of control parameters. Based on these evaluations, we demonstrate that both full physics and proxy models share similar extrema.

In addition, a constrained nonlinear optimization is applied to determine an optimal production strategy for the gas injection operation in the simplified physical setting. For an optimization model with more control parameters, when the initial guess of controls is near the optimal solution, we show that both full physics model and proxy model converge to similar optimal solution. For arbitrary initial guesses, the converged optimal strategy may differ between the proxy and the full compositional models due to a local extrema of both objective functions.

Through the optimization process in four-component system, we have shown that by providing the optimizer with the same input parameters in both the full physics model and the proxy model, the optimal solution with the proposed proxy model is usually more feasible (takes less iterations) than the full physics model. In addition, the forward simulation of the proposed proxy model is significantly cheaper (proportional to the reduction in the number of components) than the full-physics model and becomes comparable with the conventional black oil model. In our future work, we will extend the proposed model for a more realistic situation involving more governing physics.

Acknowledgments We acknowledge financial support from Xodus Group. We also would like to acknowledge the technical assistance by Mark Khait during this study.

Appendix A: Fluid and rock interactions

The simulation model in this study is a 1D homogeneous model ($K = 20$ mD), 1000 m long with one injection well on the left and one production well on the right boundaries. The finite volume discretization is applied based on the standard Cartesian grid with the block sizes: $\Delta x = 1$ m, $\Delta y = 10$ m, $\Delta z = 1$ m. For the well model, the Peaceman formula [25] is utilized with $r_w = 0.15$ m. The injection well is controlled by a constant gas rate $q_g = 2\text{m}^3/\text{day}$. The rest of parameters are specified in tables below. For the K value model, we perform the CCE using PVTi module [7] where we generate K-value table corresponding to given

Table 5 Hydrodynamic parameters

Phase	Oil	Gas
Rock compressibility, 1/bar	10^{-5}	
Porosity	0.3	
Residual saturation (S_{jr})	0.0	0.0
End point relative permeability (K_{rje})	1.0	1.0
Saturation exponent (n_j)	2.0	2.0
Viscosity, cP (μ_j)	0.5	0.1

Table 6 Thermodynamic properties quaternary system

Components	CO_2	C1	NC4	C10
Critical pressure, bars	73.87	43.04	37.47	24.20
Critical temperature, K	304.7	190.60	419.5	626.0
Critical volume, m^3/kg-mole	0.094	0.098	0.258	0.534
Acentric factor	0.225	0.013	0.1956	0.385
Molar weight, g/mol	44.01	16.04	58.12	134.0
Binary interaction, CO_2	–	0.1	0.1	0.1
Binary interaction, C1	0.1	–	–	0.041

Table 7 Thermodynamic properties for eight-component system

Components	CO_2	C1	C2	C3	NC4	C6	C8	C15
Critical pressure, bars	73.87	43.04	48.84	42.45	37.47	30.10	28.79	17.60
Critical temperature, K	304.7	190.60	305.43	369.80	419.5	507.5	575.00	724.00
Critical volume, m^3/kg-mole	0.094	0.098	0.148	0.200	0.258	0.351	0.433	0.779
Acentric factor	0.225	0.013	0.0986	0.1524	0.1956	0.299	0.312	0.55
Molar weight, g/mol	44.01	16.04	30.07	44.097	58.12	84.00	107.00	206.00

Table 8 Quaternary system

	Quaternary system			
Compositions	CO_2	C1	NC4	C10
Initial oil compositions	0.33	0.03	0.24	0.40
Injection gas compositions	1.00	0.00	0.00	0.00

Table 9 Eight-component system

	Eight-component system							
	CO2	C1	C2	C3	NC4	C6	C8	C15
Initial Oil Compositions	0.20	0.01	0.01	0.01	0.01	0.10	0.19	0.47
Injection gas Compositions	1.00	0.00	0.00	0.00	0.00	0.00	0.00	0.00

Table 10 K-value table for quaternary system

Pressure	Compositions			
	CO2	C1	NC4	C10
40 bars	6.70	8.60	1.20	0.00085
80 bars	2.05	4.70	0.54	0.005
120 bars	1.33	2.51	0.31	0.09

Table 11 K-value table for eight-component system

Pressure	Compositions							
	CO2	C1	C2	C3	NC4	C6	C8	C15
65 bars	4.31	6.73	4.33	3.05	1.22	0.50	0.23	0.0016
100 bars	1.88	3.25	2.12	1.56	0.95	0.48	0.27	0.08
140 bars	1.21	1.38	0.99	0.81	0.65	0.45	0.33	0.12

initial compositions in Table 10. The *K*-value table is present as a function of pressure with three pressure values employed (see Tables 10 and 11 for details).

For the *K*-value model, we perform the CCE using PVTi module [7], where we generate a *K*-value table corresponding to given initial compositions in Tables 8 and 9. The *K*-value table is present as a function of pressure with three pressure values employed (see Table 10 and 11 for details).

References

1. Chapman, W., Gubbins, K., Jackson, G., Radosz, M.: Saft: Equation-of-state solution model for associating fluids. Fluid Phase Equilib. **52**, 31–38 (1989)
2. Coats, K.H.: An equation of state compositional model. SPE J. **20**(05), 363–376 (1980)
3. Collins, D., Nghiem, L., Li, Y.K., Grabonstotter, J.: An efficient approach to adaptive- implicit compositional simulation with an equation of state SPE Journal 15133-PA (1992)
4. Ettehadtavakkol, A., Lake, L.W., Bryant, S.L.: Co2-eor and storage design optimization. Int. J. Greenhouse Gas Control **25**, 79–92 (2014)
5. Ganapathy, C., Chen, Y., Voskov, D.: Multiscale reconstruction of compositional transport. In: ECMOR 2018-16Th European Conference on the Mathematics of Oil Recovery (2018)
6. Ganapathy, C., Voskov, D.: Multiscale reconstruction in physics for compositional simulation. J. Comput. Phys. **375**, 747–762 (2018)
7. Geoquest: PVTI Reference Manual. Schlumberger, Houston (2008)
8. Iranshahr, A., Chen, Y., Voskov, D.V.: A coarse-scale compositional model. Comput. Geosci. **18**(5), 797–815 (2014)
9. Iranshahr, A., Voskov, D., Tchelepi, H.: Generalized negative flash method for multiphase muticomponent systems. Fluid Phase Equilib. **299**, 272–283 (2010)
10. Iranshahr, A., Voskov, D., Tchelepi, H.: A negative-flash tie-simplex approach for multiphase reservoir simulation. SPE J. **18**(6), 1140–1149 (2013)
11. Jenny, P., Lee, S.H., Tchelepi, H.A.: Multi-scale finite-volume method for elliptic problems in subsurface flow simulation. J. Comput. Phys. **187**(1), 47–67 (2003)
12. Khait, M., Voskov, D.: Adaptive parameterization for solving of thermal/compositional nonlinear flow and transport with buoyancy. SPE J. **33**(02), 522–534 (2018). SPE-182685-PA
13. Khait, M., Voskov, D.V.: Operator-based linearization for general purpose reservoir simulation. J. Pet. Sci. Eng. **157**, 990–998 (2017)
14. Kontogeorgis, G.M., Voutsas, E.C., Yakoumis, I.V., Tassios, D.P.: An equation of state for associating fluids. Ind. Eng. Chem. Res. **35**(11), 4310–4318 (1996)
15. Kwak, D.H., Kim, J.K.: Techno-economic evaluation of CO_2 enhanced oil recovery (EOR) with the optimization of CO_2 supply. Int. J. Greenhouse Gas Control **58**, 169–184 (2017)
16. Lake, L.W.: Enhanced Oil Recovery. Prentice-Hall, Upper Saddle River (1989)
17. Lucia, A., Henley, H., Thomas, E.: Multiphase equilibrium flash with salt precipitation in systems with multiple salts. Chem. Eng. Res. Des. **93**, 662–674 (2015)
18. MathWorks: Matlab optimization toolbox (2018)
19. McCoy, S.T., Rubin, E.S.: The effect of high oil prices on EOR project economics. Energy Procedia **1**(1), 4143–4150 (2009). Greenhouse Gas Control Technologies 9
20. Michelsen, M.L.: The isothermal flash problem. Part i. Stability. Fluid Phase Equilib. **9**(1), 1–19 (1982)
21. Michelsen, M.L.: The isothermal flash problem. Part ii. Phase-split calculation. Fluid Phase Equilib. **9**(1), 21–40 (1982)
22. Orr, F.M.: Theory of Gas Injection Process. Tie-Line Publications, Denmark (2007)
23. Pan, H., Tchelepi, H.A.: Compositional flow simulation using reduced-variables and stability-analysis bypassing. In: SPE Reservoir Simulation Symposium. SPE-142189-MS (2011)
24. Paterson, D., Michelsen, M., Yan, W., Stenby, E.: Extension of modified rand to multiphase flash specifications based on state functions other than (t,p). Fluid Phase Equilib. **458**, 288–299 (2018)
25. Peaceman, D.W.: Interpretation of well-block pressures in numerical reservoir simulation. SPE J. **18**(03), 183–194 (1978). SPE-6893-PA
26. Peng, D.Y., Robinson, D.B.: A new two-constant equation of state. Ind. Eng. Chem. Fundam. **15**(1), 59–64 (1976)
27. Rannou, G., Voskov, D., Tchelepi, H.: Tie-line-based k-value method for compositional simulation. SPE J. **18**(6), 1112–1122 (2013)
28. Rasmussen, C.P., Krejbjerg, K., Michelsen, M.L., Bjurstrøm, K.E.: Increasing the computational speed of flash calculations with applications for compositional, transient simulations. SPE Reserv. Eval. Eng. **9**(01), 32–38 (2006). SPE-84181-PA
29. Rubin, E.S., Chen, C., Rao, A.B.: Cost and performance of fossil fuel power plants with co2 capture and storage. Energy Policy **35**(9), 4444–4454 (2007)
30. Salehi, A.: Upscaling of Compositional Flow Simulation Based on a Non-Equilibrium Formulation. Stanford University, Ph.D. thesis (2016)
31. Soave, G.: Equilibrium constants from a modified Redlich-Kwong equation of state. Chem. Eng. Sci. **27**(6), 1197–1203 (1972)
32. Tayari, F., Blumsack, S., Johns, R.T., Tham, S., Ghosh, S.: Techno-economic assessment of reservoir heterogeneity and permeability variation on economic value of enhanced oil recovery by gas and foam flooding. J. Pet. Sci. Eng. **166**, 913–923 (2018)
33. Voskov, D., Entov, V.: Problem of oil displacement by gas mixtures. Fluid Dyn. **36**(2), 269–278 (2001)
34. Voskov, D., Henley, H., Lucia, A.: Fully compositional multi-scale reservoir simulation of various CO_2 sequestration mechanisms. Comput. Chem. Eng. **96**, 183–195 (2017)

35. Voskov, D., Tchelepi, H.: Compositional space parameterization for flow simulation. In: SPE Reservoir Simulation Symposium Proceedings, pp. 100–110 (2007)
36. Voskov, D.V.: Operator based linearization approach for modeling of multiphase multicomponent flow in porous media. J. Comput. Phys. **337**, 275–288 (2017)
37. Wei, N., Li, X., Dahowski, R.T., Davidson, C.L., Liu, S., Zha, Y.: Economic evaluation on CO_2-EOR of onshore oil fields in china. Int. J. Greenhouse Gas Control **37**, 170–181 (2015)
38. Zaydullin, R., Voskov, D., Tchelepi, H.A.: Nonlinear formulation based on an equation-of-state free method for compositional flow simulation. Society of Petroleum. SPE Journal **18**(02), 264–273 (2012). SPE-146989-PA
39. Zhou, H., Lee, S.H., Tchelepi, H.A.: Multiscale finite-volume formulation for saturation equations. SPE J. **17**(01), 198–211 (2012). SPE-119183-PA